frontiers | Frontiers in Pharmacology

TYPE Original Research
PUBLISHED 27 March 2025
DOI 10.3389/fphar.2025.1367991

OPEN ACCESS

EDITED BY
Ravinder Abrol,
California State University, Northridge, United States

REVIEWED BY
Vsevolod V. Gurevich,
Vanderbilt University, United States
Emma T. van der Westhuizen,
University of Melbourne, Australia

*CORRESPONDENCE
David A. Sykes,
david.sykes@nottingham.ac.uk
Stephen J. Briddon,
stephen.briddon@nottingham.ac.uk
Dmitry B. Veprintsev,
dmitry.veprintsev@nottingham.ac.uk

RECEIVED 09 January 2024
ACCEPTED 24 February 2025
PUBLISHED 27 March 2025

CITATION
Harwood CR, Sykes DA, Redfern-Nichols T, Underwood O, Nicholson C, Khoshgrudi AN, Koers EJ, Ladds G, Briddon SJ and Veprintsev DB (2025) Agonist efficacy at the β_2AR is driven by the faster association rate of the G_s protein.
Front. Pharmacol. 16:1367991.
doi: 10.3389/fphar.2025.1367991

Agonist efficacy at the β_2AR is driven by the faster association rate of the G_s protein

Clare R. Harwood[1,2], David A. Sykes[1,2,3]*, Theo Redfern-Nichols[4], Owen Underwood[3], Colin Nicholson[1,2], Armin N. Khoshgrudi[1,2], Eline J. Koers[1,2], Graham Ladds[2,4], Stephen J. Briddon[1,2]* and Dmitry B. Veprintsev[1,2,3]*

[1]Division of Physiology, Pharmacology and Neuroscience, School of Life Sciences, University of Nottingham, Nottingham, United Kingdom, [2]Centre of Membrane Proteins and Receptors (COMPARE), University of Birmingham and University of Nottingham, Nottingham, United Kingdom, [3]Z7 Biotech Ltd., Nottingham, United Kingdom, [4]Department of Pharmacology, University of Cambridge, Cambridge, United Kingdom

Introduction: The β_2-adrenoceptor (β_2AR) is a class A G protein-coupled receptor (GPCR). It is therapeutically relevant in asthma and chronic obstructive pulmonary disease (COPD), where β_2AR agonists relieve bronchoconstriction. The β_2AR is a prototypical GPCR for structural and biophysical studies. However, the molecular basis of agonist efficacy at the β_2AR is not understood. We hypothesised that the kinetics of GPCR–G protein interactions could play a role in determining ligand efficacy. By studying a range of agonists with varying efficacy, we examined the relationship between ligand-induced mini-G_s binding to the β_2AR and ligand efficacy, along with the ability of individual ligands to activate the G protein in cells.

Methods: We used NanoBRET technology to measure ligand-induced binding of purified Venus-mini-G_s to β_2AR-nLuc in membrane preparations under both equilibrium and kinetic conditions. In addition, we examined the ability of these β_2AR agonists to activate the heterotrimeric G_s protein, measured using the G_s-CASE protein biosensor in living cells. This assay detects a reduction in NanoBRET between the nano-luciferase (nLuc) donor on the Gα subunit and Venus acceptor on the Gγ upon G_s protein activation.

Results: The 12 β_2AR agonists under study revealed a broad range of ligand potency and efficacy values in the cellular G_s-CASE assays. Kinetic characterisation of mini-G_s binding to the agonist β_2AR complex revealed a strong correlation between ligand efficacy values (E_{max}) and mini-G_s affinity (K_d) and its association rate (k_{on}). In contrast, there was no correlation between ligand efficacy and reported ligand dissociation rates (or residence times).

Conclusion: The association rate (k_{on}) of the G protein to the agonist β_2AR complex is directly correlated with ligand efficacy. These data support a model in

which higher-efficacy agonists induce the β_2AR to adopt a conformation that is more likely to recruit G protein. Conversely, these data did not support the role of agonist binding kinetics in determining the molecular basis of efficacy.

KEYWORDS

G protein-coupled receptor, β2-adrenoceptor, efficacy, kinetics, association rate kon, dissociation rate koff

Introduction

G protein-coupled receptors (GPCRs) are the largest family of membrane proteins in the human genome and are responsible for modulating a broad range of hormonal, neurological, and immune responses. GPCR-directed therapeutics currently target over 100 diverse receptors and represent 34% of all US Food and Drug Administration (FDA)-approved drugs, making them the most widely targeted receptors (Hauser et al., 2017). Despite their therapeutic importance, the molecular basis of ligand efficacy—the ability of a drug to affect GPCR signal transduction—is not fully understood. It is hoped that a deeper understanding of the molecular basis of efficacy will aid in more rational drug design.

The process of GPCR activation involves agonist binding, a ligand-induced conformational change in the receptor and the subsequent recruitment and activation of a G protein. Several studies have implicated ligand residence time in the molecular basis of efficacy at GPCRs. For example, a positive correlation has been observed between the efficacy of seven agonists at the muscarinic M3 receptor and 10 agonists at the adenosine A_{2A} receptor (A_{2A}R) with their ligand residence time (Sykes et al., 2009b; Guo et al., 2012). Conversely, no correlation between efficacy and residency time was found for ligands at the adenosine A_1 receptor (Louvel et al., 2014).

Biophysical studies have shown that agonists shift the receptor conformational landscape in favour of a unique active conformation, compared to the unliganded state (Deupi and Kobilka, 2010; Mary et al., 2012; Nygaard et al., 2013), but how conformational differences in a population translate to greater or lesser signalling responses remains to be fully elucidated. Structural studies have found little differences in GPCR conformations adopted by ligand-bound GPCR–G-protein complexes (Masureel et al., 2018; Zhang et al., 2020). However, using nuclear magnetic resonance (NMR), Liu et al. (2012) showed efficacy-dependent differences in the conformational state of β_2AR bound to different agonists prior to G protein binding. Similar results have been observed for the β_1AR (Grahl et al., 2020; Jones et al., 2024) and A_{2A}R (Ye et al., 2016). Alternatively, some studies (Nikolaev et al., 2006; Gregorio et al., 2017) show correlations between ligand efficacy and the rate of GPCR and G protein activation, suggesting a key role for G protein binding kinetics in dictating pharmacological efficacy.

Consequentially, we aimed to delineate the roles of ligand binding and receptor–G protein binding kinetics in agonist efficacy. We focused on the β_2-adrenoceptor (β_2AR), a prototypical class A GPCR, which is one of the most structurally, functionally, and therapeutically well-characterised GPCRs. The β_2AR is also an essential target in the treatment of asthma and COPD, and as a result, a wide range of clinically used agonists of varying efficacies have been developed to target the β_2AR, which could be utilised in this study.

G proteins are heterotrimeric, consisting of α, β, and γ subunits The Gα subunit comprises of a helical and GTPase domain. Full-length heterotrimeric G proteins are dynamic complexes that are difficult to isolate. To overcome this, we chose to utilise mini-G proteins (Carpenter and Tate, 2016) as tools to study the dynamics of β_2AR activation. The mini-G_s protein is the isolated GTPase domain of the Gα subunit, which has been engineered with several thermostabilising mutations that make it a rigid protein, locked in its active state, as shown in the agonist-bound A_{2A}R-mini-G_s structure (Carpenter et al., 2016; Carpenter and Tate, 2017). These mini-G proteins have also been converted into convenient probes that report the active state of a GPCR (Wan et al., 2018).

We investigated the binding kinetics and affinity of fluorescently labelled (Venus-fused) mini-G_s proteins for the β_2AR in complex with a set of agonists of varying efficacy, from partial to full agonists. In addition, we correlated ligand binding affinities, residence times, and efficacy at the level of heterotrimeric G_s protein activation for these agonists.

Materials, instruments and software

Materials

The T-REx™-293 Cell Line was obtained from Invitrogen (CA, United States). T75 and T175 mammalian cell culture flasks were purchased from Fisher Scientific (Loughborough, United Kingdom). All cell culture reagents, including Hank's balanced salt solution (HBSS), phosphate-buffered saline (PBS), and foetal calf serum (FCS), were purchased from Sigma Aldrich (Gillingham, United Kingdom), except for blasticidin, which was obtained from Gibco™ (MA, United States), and Zeocin™. Polyethylenimine (PEI) (25 kDa) was obtained from Polysciences Inc. (PA, United States), and the culture plates were obtained from Greiner Bio-One (code 655098 Kremsmünster, Austria).

HisTrap FF crude 5-mL columns were obtained from GE Healthcare (IL, United States). Vivaspin protein concentrators were obtained from Sartorius (Göttingen, Germany). Slide-A-Lyzer Dialysis Cassettes, NuPAGE LDS Sample Buffer, NuPAGE 4%–12% Bis-Tris 15 × 1.0 mm well gels, NuPAGE MOPS SDS Running Buffer, PageRuler Prestained Protein Ladder, were all obtained from Thermo Fisher (MA, United States).

Salmeterol was obtained from Tocris (Bristol, U.K). Formoterol hemifumarate was obtained from APExBIO (TX, United States), and BI-167-107 was obtained from Boehringer Ingelheim (Ingelheim, Germany). Compound 26 was a gift from Novartis. (±)-Epinephrine hydrochloride, noradrenaline, salbutamol

hemisulfate, and isoprenaline hydrochloride were purchased from Sigma-Aldrich (Gillingham, United Kingdom). Dobutamine hydrochloride was obtained from Merck Life Sciences, UK. Isoxsuprine hydrochloride, ritodrine hydrochloride, and tulobuterol were obtained from CliniSciences Limited. Nano-Glo luciferase substrate was obtained from Promega (WI, United States). All other chemicals were purchased from Sigma-Aldrich (Gillingham, United Kingdom).

Instruments and software

BMG PHERAstar FSX plate reader (BMG Labtech, Offenburg, Germany), fitted with BRET1 plus optic module (ex. 475/30 nm, em. 535/30 nm) and MARS software, was purchased from BMG Labtech (Offenburg, Germany). GraphPad Prism 9 was purchased from GraphPad Software (San Diego, United States). Microsoft Excel™ XP was purchased from Microsoft (Washington, United States).

Methods

Molecular biology

The construct pcDNA4TO-TwinStrep (TS)-SNAP-β_2AR was generated through the amplification of the SNAP and β_2AR sequences from the pSNAPf-ADRB2 plasmid (NEB) and inserted into pcDNA4TO-TS using Gibson assembly (Heydenreich et al., 2017). pcDNA4TO-TS-SNAP-β_2AR-nLuc was generated by Dr. Brad Hoare through the amplification of pcDNA4TO-TS-SNAP-β_2AR and nanoLuc, with the insertion of nanoLuc into pcDNA4TO-TS-SNAP-β_2AR via Gibson assembly. Both constructs used a signal peptide based on the $5HT_{3A}$ receptor to increase protein folding and expression. The CASE G_s (or G_s-CASE) protein constructs were designed and optimised by the Schulte Lab (Schihada et al., 2021) and were obtained from Addgene. Mammalian Venus-fused mini-G_s constructs were a kind gift from Nevin Lambert (Wan et al., 2018). For the bacterial expression of Venus-mini-G_s and mini-G_s, protein encoding DNA sequences were amplified from the corresponding mammalian constructs and inserted into the pJ411 vector containing MKK-HIS10-TEV N-terminal tag (Sun et al., 2015) via Gibson assembly, yielding the constructs MKK-HIS10-TEV-mini-G_s and MKK-HIS10-TEV-Venus-mini-G_s.

Transfection and mammalian cell culture

pcDNA4TO-TS-SNAP-β_2AR or pcDNA4TO-TS-SNAP-β_2AR-nLuc was stably transfected into T-REx™-293 cells (Invitrogen) using PEI. A stable mixed population was selected by resistance to 5 μg/mL blasticidin and 20 μg/mL zeocin. Stable cell lines were maintained in high-glucose DMEM (Sigma D6429) with 10% FBS, 5 μg/μL blasticidin, and 20 μg/μL zeocin at 37°C in a humidified atmosphere of 5% CO_2. When ~70% confluent, TS-SNAP-β_2AR or TS-SNAP-β_2AR-nLuc expression was induced with 1 μg/mL tetracycline. Cells were left to express for 50 h before harvesting for assays. The T-REx™-293 pcDNA4TO-TS-SNAP-β_2AR-CASE G_s stable cell line was generated by stably transfecting the CASE G_s constructs into the T-REx™-293 pcDNA4TO-TS-SNAP-β_2AR using PEI. A mixed population stable cell line was generated by selection with 500 μg/mL G418, and then a single colony population was generated via FACS.

Membrane preparations of TS-SNAP-β_2AR-nLuc

For membrane preparation, all steps were conducted at 4°C to avoid tissue degradation. Cell pellets were thawed and re-suspended using ice-cold buffer containing 10 mM HEPES and 10 mM EDTA (pH 7.4). The suspension was homogenised using an electrical homogeniser (ULTRA-TURRAX, IKA-Werke GmbH, Germany) and subsequently centrifuged at 1,200 × g for 5 min. The pellet obtained, containing cell nucleus and other heavy organelles, was discarded, and the supernatant was centrifuged for 30 min at 48,000 × g at 4°C (Beckman Avanti J-251 Ultra-centrifuge; Beckman Coulter). The supernatant was discarded, and the pellet was re-suspended in the same buffer (10 mM HEPES and 10 mM EDTA; pH 7.4) and centrifuged again for 30 min as described above. Finally, the supernatant was discarded, and the pellet was re-suspended in ice-cold 10 mM HEPES and 0.1 mM EDTA (pH 7.4). Protein concentration determination was carried out using the bicinchoninic acid assay kit (Sigma-Aldrich) with BSA as the standard. The final membrane suspension was aliquoted and maintained at −80°C until required for the assays.

Solubilisation of the TS-SNAP-β_2AR or TS-SNAP-β_2AR-nLuc

TS-SNAP-β_2AR or TS-SNAP-β_2AR-nLuc was solubilised from stably transfected T-REx™-293 cell membranes, as described previously (Harwood et al., 2024). Solubilisation was carried out using 1% DDM (w/v) in 20 mM HEPES, 5% (v/v) glycerol, and 150 mM NaCl, pH 8, at 4°C for 2–3 h. Samples were clarified by ultracentrifugation at 4°C for 1 h at 100,000 × g.

Production of mini-G_s

His-TEV-Venus-mini-G_s and His-TEV-mini-G_s were expressed in NiCo21(DE3) *E. coli*, cultured in Terrific Broth (Gibco). 1L cultures were induced with 1 mM isopropyl β-D-1-thiogalactopyranoside (IPTG) at OD = 0.6 and incubated for a further 20 h at 20°C and 225 RPM. Pellets from 1L cultures were thawed on ice, and re-suspended in 50 mL lysis buffer (20 mM HEPES, pH 7.5, 500 mM NaCl, 40 mM imidazole, 10% glycerol, 8 mM β-mercaptoethanol (BME), 1 μM guanosine diphosphate (GDP), complete protease inhibitors (Roche), DNase I, and lysozyme) using a Dounce homogeniser. Lysis occurred on ice via sonication, using a Vibra-Cell probe sonicator with 5 × 10-s pulses, 30 s apart. The lysate was loaded onto the HisTrap FF crude 5-mL column, using ÄKTA™ start protein purification system at a flow rate of 5 mL/min. The system and column had been equilibrated with 10 column volumes (CV) of buffer A (20 mM HEPES, 500 mM NaCl, 40 mM imidazole, 10% glycerol, 8 mM BME, and 1 μM GDP). Unbound protein was washed out with

10 CV of buffer A. Bound protein was then eluted over an 8 CV gradient of 0% to 100% buffer B at a flow rate of 5 mL/min (Buffer B = 20 mM HEPES, 500 mM NaCl, 400 mM imidazole, 10% glycerol, 8 mM BME, and 1 μM GDP). The presence of His-TEV-Venus-mini-G_s and His-TEV-mini-G_s was confirmed by SDS-PAGE analysis and InstantBlue staining for protein. Pooled elution fractions were then concentrated using 10,000 or 30,000 molecular weight cutoff (MWCO) Vivaspin protein concentrators by centrifugation at 3000 × g and 4°C for 15-min intervals over 2–3 h. Protein was exchanged into assay buffer using Slide-A-Lyzer 10,000 or 30,000 MWCO dialysis cassettes for untagged and Venus-tagged mini-G_s protein samples, respectively. Dialysis occurred overnight at 4°C under constant stirring. The assay buffer consisted of 20 mM HEPES, 150 mM NaCl, 10% glycerol, 8 mM BME, and 1 μM GDP. The purified mini-G_s protein was flash-frozen using liquid nitrogen and stored at −80°C.

Membrane-based TS-SNAP-β_2AR-Venus-mini-G_s NanoBRET binding assays

The assay buffer, consisting of HBSS (Sigma H8264) containing 10 mM HEPES, 0.1% BSA, and 0.1% ascorbic acid, pH 7.4, was used in all NanoBRET assays. For recruitment assays, varying concentrations of β_2AR agonists were used to recruit Venus-mini-G_s to the TS-SNAP-β_2AR. Assays were run in 50 μL volumes in white 384-well OptiPlate (Revvity). Receptor, ligand, 0.3 μM mini-G_s proteins, and 10 μM furimazine were added to the plate and incubated for 60 min at room temperature before reading on PHERAstar FSX using the BRET1 module. For kinetic assays, in which the affinity of Venus-mini-G_s for the agonist-bound TS-SNAP-β_2AR-nLuc receptors was measured over time, assays were run in 50 μL volumes in white 384-well OptiPlate. Varying concentrations (10–300 nM) of Venus-mini-G_s were added to assay plates. TS-SNAP-β_2AR membranes were pre-incubated with saturating concentrations (100x EC_{50}) of selected β_2AR agonists and furimazine for 15 min prior to addition to the plate. TS-SNAP-β_2AR membranes were added to the plate offline and mixed with the Venus-mini-G_s on a plate shaker (MixMate, Eppendorf) at 600 RPM for 10 s. The mixture was then immediately read on PHERAstar FSX as described above, with readings taken over a period of 240 min.

G_s-CASE activation assays

For G_s-CASE activation assays, a single population of T-REx™-293 stably expressing pcDNA4TO-TS-SNAP-β_2AR and CASE G_s was plated at 50,000 cells/well in 96-well plates, in a volume of 100 μL, and induced for 48 h with 1 μg/mL tetracycline at 37°C and 5% CO_2. Plates were washed once with 100 μL/well assay buffer (HBSS containing 10 mM HEPES, 0.1% BSA, and 0.1% ascorbic acid) prior to the addition of 90 μL/well of assay buffer containing 10 μM furimazine, diluted in assay buffer, to achieve a final concentration of 8 μM. The plates were incubated at 37°C and 5% CO_2 for 20 min. A white back seal was placed on the underside of the plate, and luminescence was read on a PHERAstar FSX using the BRET1 module for 3 min to establish a baseline BRET signal. The plate reader was then paused, and 10 μL of ×10 ligand dilutions were added accordingly. Readings were taken over a period of 30 min.

Mathematical modelling

The previously described ordinary differential model (ODE) of the cubic ternary complex model (Weiss et al., 1996), with additional reactions to simulate the G protein activation cycle, was used (Woodroffe et al., 2009; Bridge et al., 2018). The model, encoded in COPASI (Hoops et al., 2006), includes ligand binding, receptor activation, G protein binding, and the G protein cycle, whereby the model output is activated G protein $G\alpha_{GTP}$ and receptor occupancy (Bridge et al., 2018). Prior to the addition of the ligand, we first compute the system for 10^6 s. To enable the simulation of the data, the cooperativity factor β (see Supplementary Figure 7; Supplementary Table 3) was varied, and simulations were performed. Steady state was reached after 5 min, and outputs are shown after 10 min.

Data analysis

All non-linear regression and statistical analyses were performed using GraphPad Prism 9. Multiple replicates were combined, such as TR-FRET equilibrium binding curves and mini-G_s equilibrium recruitment curves, as shown in Supplementary Material. Data points for each replicate were normalised to the maximum value obtained for each ligand in each experiment. Competition ligand-binding data were fitted to a one-site model (Equation 1).

$$Y = \frac{Bottom + (Top - Bottom)}{\left(1 + 10^{(x - LogIC_{50})}\right)}, \quad (1)$$

where Y is the binding of tracer, x = Log [ligand], IC_{50} is the concentration of the competing ligand that displaces 50% of radioligand-specific binding.

CASE G_s activation data from individual experiments were fitted to sigmoidal (variable slope) curves using a "four-parameter logistic equation" (Equation 2):

$$Y = Bottom + \frac{(Top - Bottom)}{1 + 10^{(logEC50 - X)*Hillslope}}, \quad (2)$$

where Bottom is the plateaus of the agonist concentration response curve and Top is the basal response (fixed to 1). $LogEC_{50}$ is the concentration of the agonist that produces a half-maximal effect, and the Hillslope is the unitless slope factor or Hillslope, which was fixed to −1.

Mini-G_s association data were fitted to a global fitting model (Equation 3) using GraphPad Prism 9.2 to simultaneously calculate k_{on} and k_{off} using the following equations, where k_{obs} equals the observed rate of association and L is the concentration of mini-G_s.

$$\begin{aligned} K_d &= \frac{k_{off}}{k_{on}}, \\ L &= Hotnm*1e-9, \\ K_{ob} &= k_{on}*L + k_{off}, \\ Occupancy &= L/(L + K_d), \\ Y_{max} &= Occupancy*B_{max}, \\ drift &= B_{max}*\exp(-drift*X), \\ Y &= (Y_{max}*(1 - \exp(-1*k_{ob}*X)))*drift. \end{aligned} \quad (3)$$

Saturation binding curves for Venus-mini-G_s binding to the agonist TS-SNAP-β_2AR-nLuc were fitted to a one-site specific binding model according to Equation 4. The final K_d values were taken as an average of K_d values from individual specific curve fits.

$$Y = \frac{Bmax*X}{(K_d + X)}, \quad (4)$$

where Y is the specific binding, K_d is the equilibrium dissociation constant of the labelled ligand (in this case, Venus-mini-G_s), and x represents [Venus-mini-G_s] in nM.

Statistical analysis

Pearson's correlation coefficient was used to investigate correlations between mini-G_s recruitment, CASE-G_s activation, mini-G_s binding K_d, k_{on} and k_{off} values, and literature p$K_{i/d}$. Deming regression was applied to determine the line of best fit while accounting for errors in observations on both the x- and y-axes. All statistical analyses were performed in GraphPad Prism 9, and $p < 0.05$ was considered statistically significant.

Results

Characterisation of β_2AR agonist efficacy for G_s activation

To produce a suitable dataset for analysis, we chose 12 β_2AR agonists anticipated to have a diverse range of efficacies, affinities, and ligand binding kinetics. We first characterised the efficacy of these compounds in activating the heterotrimeric G_s protein using a NanoBRET-based biosensor (Schihada et al., 2021; Harwood et al., 2024). In this assay format, G_s protein activation results in a decrease in the NanoBRET signal as the nLuc-labelled α-subunit of the G_s protein dissociates from the Venus-labelled γ-subunit. These experiments are summarised in Figures 1A–C and Table 1.

The Gs-CASE assay functions as a non-amplified system, showing very distinct differences in measurable efficacy between full and partial agonists. The concentration-response curves for formoterol (full) and tulobuterol (partial agonist) are shown in Figure 1A. A broad range of potencies was observed

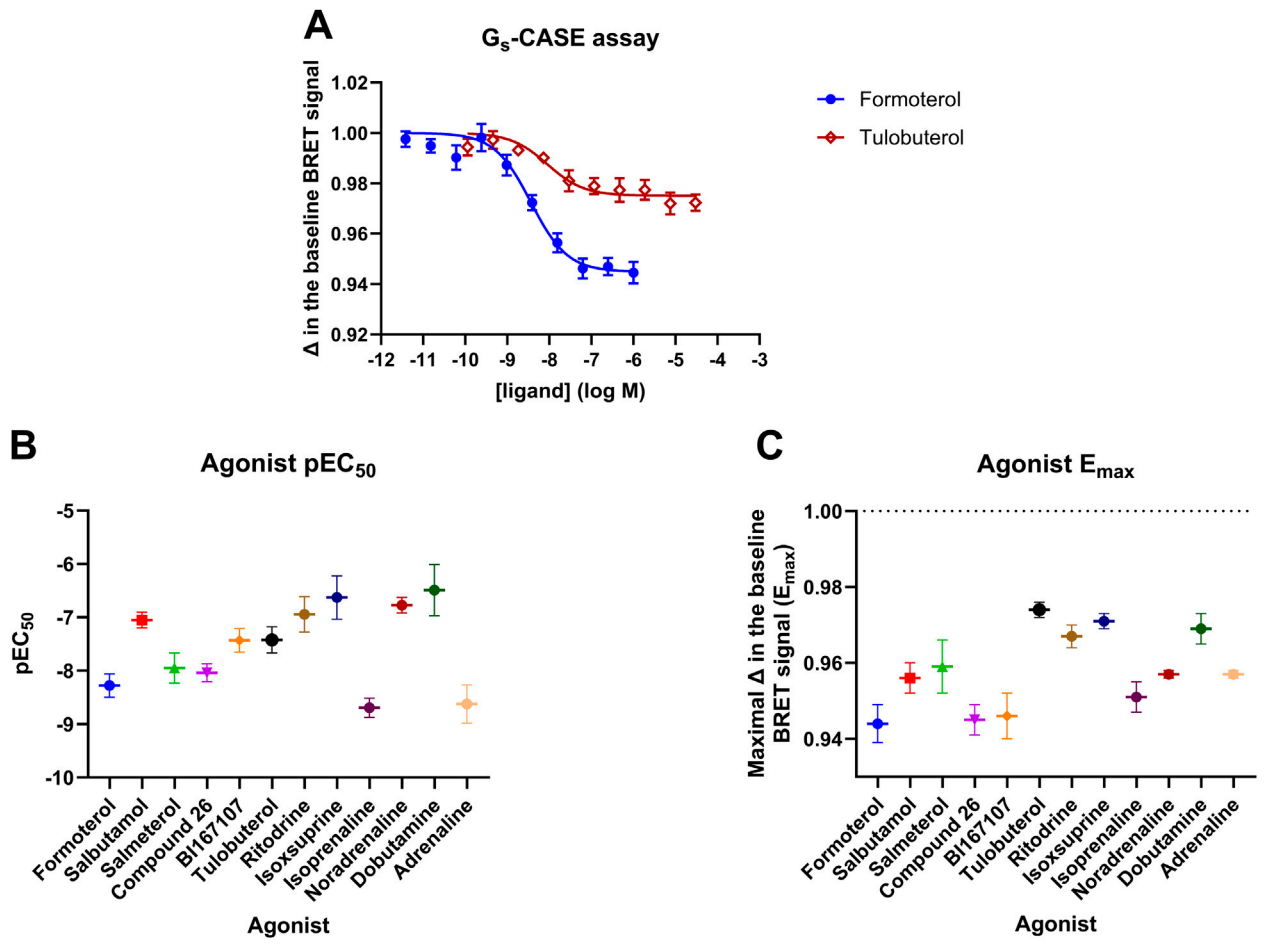

FIGURE 1
T-REx™-293-SNAP-β_2AR G_s-CASE activation assay. **(A)** Concentration-response curves are shown for the full agonist formoterol and the partial agonist tulobuterol. The Gs-CASE baseline BRET signal was set to 1 for normalisation purposes. The response to each agonist is expressed as a fractional change relative to the basal response. Response data are representative of three or more experiments. **(B)** Gs-CASE pEC_{50} and **(C)** E_{max} values are shown for the 12 agonists. Data are presented as the mean ± SEM of three or more experiments.

TABLE 1 Summary of efficacy and potency values obtained for β_2AR agonists in the G_s-CASE activation assay.

	Gs-CASE assay	
	pEC_{50}	E_{max}
Formoterol	8.28 ± 0.22	0.944 ± 0.005
Salbutamol	7.05 ± 0.15	0.956 ± 0.004
Salmeterol	7.95 ± 0.28	0.959 ± 0.007
Compound 26	8.03 ± 0.17	0.945 ± 0.004
BI167107	7.43 ± 0.22	0.946 ± 0.006
Tulobuterol	7.42 ± 0.25	9.974 ± 0.002
Ritodrine	6.95 ± 0.33	0.967 ± 0.003
Isoxsuprine	6.63 ± 0.41	0.971 ± 0.002
Isoprenaline	8.69 ± 0.18	0.951 ± 0.004
Noradrenaline	6.77 ± 0.15	0.957 ± 0.001
Dobutamine	6.49 ± 0.48	0.969 ± 0.004
Adrenaline	8.62 ± 0.36	0.957 ± 0.001

The T-REx™-293-SNAP-β_2AR CASE G_s stable cell line was induced with 1 μg/mL tetracycline for 48 h. The Gs-CASE response of each agonist was expressed as a fractional change in the basal response. Values are presented as the mean ± SEM of three or more experiments.

for the 12 tested ligands, with pEC_{50} values ranging from 6.49 ± 0.48 for dobutamine to 8.69 ± 0.18 for isoprenaline (see Figure 1B; Table 1). Figure 1C shows a range of efficacy values for each agonist, represented by E_{max} (maximal decrease in basal BRET) values, with the lowest efficacy agonists being tulobuterol and isoxsuprine and the highest being formoterol and Compound 26.

Validation of mini-G_s proteins as tools for probing G_s protein binding

In order to investigate the mechanism underlying the differences in efficacy, we expressed and purified fluorescently labelled mini-G_s proteins from *E.* coli (Supplementary Figure 1); our aim was to probe the affinity and binding kinetics of Venus-mini-G_s protein for the agonist-bound β_2AR–nLuc complex using NanoBRET. Figure 2A shows that all 12 agonists recruited Venus-mini-G_s protein to β_2AR-nLuc in HEK cell membranes in a concentration-dependent manner, with varying E_{max} and pEC_{5o} values (Table 2). Moreover, Figure 2B reveals a strong correlation ($R^2 = 0.80$, $p = 0.0001$) between E_{max} values for mini-G_s recruitment and E_{max} values for G_s-CASE activation, further validating these assays as effective tools for investigating β_2AR–G_s interactions.

Investigating the kinetics of mini-G_s protein binding to the β_2AR in complex with agonists of varying efficacies

We established a kinetic NanoBRET binding assay to measure Venus-mini-G_s protein recruitment to β_2AR-nLuc in membrane preparations. To achieve this, we pre-incubated receptor-containing membranes with a saturating concentration (×100 EC_{50}) of each β_2AR agonist, as characterised above. The pre-incubated membranes were then added to a plate containing various concentrations of Venus-mini-G_s protein, and we measured the association between these two proteins using NanoBRET (Figure 3; Table 3). Both association and dissociation rates (k_{on} and k_{off}) of Venus-mini-G_s for agonist β_2AR-nLuc could be obtained by analysing the observed association kinetics (Table 3). These studies showed that the full agonists, isoprenaline ($k_{on} = 3.00 \pm 0.1 \times 10^5$ M^{-1} min^{-1}) and adrenaline ($k_{on} = 3.06 \pm 0.15 \times 10^5$ M^{-1} min^{-1}), induce faster recruitment of the mini-G_s protein than the partial agonists, ritodrine ($k_{on} = 6.13 \pm 0.75 \times 10^4$ M^{-1} min^{-1}) and isoxsuprine ($k_{on} = 4.97 \pm 0.29 \times 10^4$ M^{-1} min^{-1}). k_{off} values were similar for all ligands, with all values within the range of 0.0070–0.0113 min^{-1}. We also conducted these mini-G_s kinetics studies on β_2AR-nLuc extracted into DDM detergent micelles, using 6 of the 12 ligands (Supplementary Figure 2; Supplementary Table 1) and observed similar results.

To probe the binding affinity of the Venus mini-G_s protein to the agonist β_2AR–nLuc complex, we added ligands in excess (×100 reported pEC_{50} determined in the mini-G_s recruitment assay, see above) and incubated with the membrane fraction expressing β_2AR-nLuc for 15 min prior to the addition of Venus-labelled mini-G_s (Figure 4). The resulting affinity (pK_d) values are summarised in Table 3, which ranged from 24 nM for the full agonist isoprenaline to 193 nM for the partial agonist isoxsuprine. These data also showed a difference in the maximum amount of mini-G_s protein (E_{max}) recruited over the limited concentration range studied (300–10 nM), with full agonists exhibiting higher recruitment compared to partial agonists.

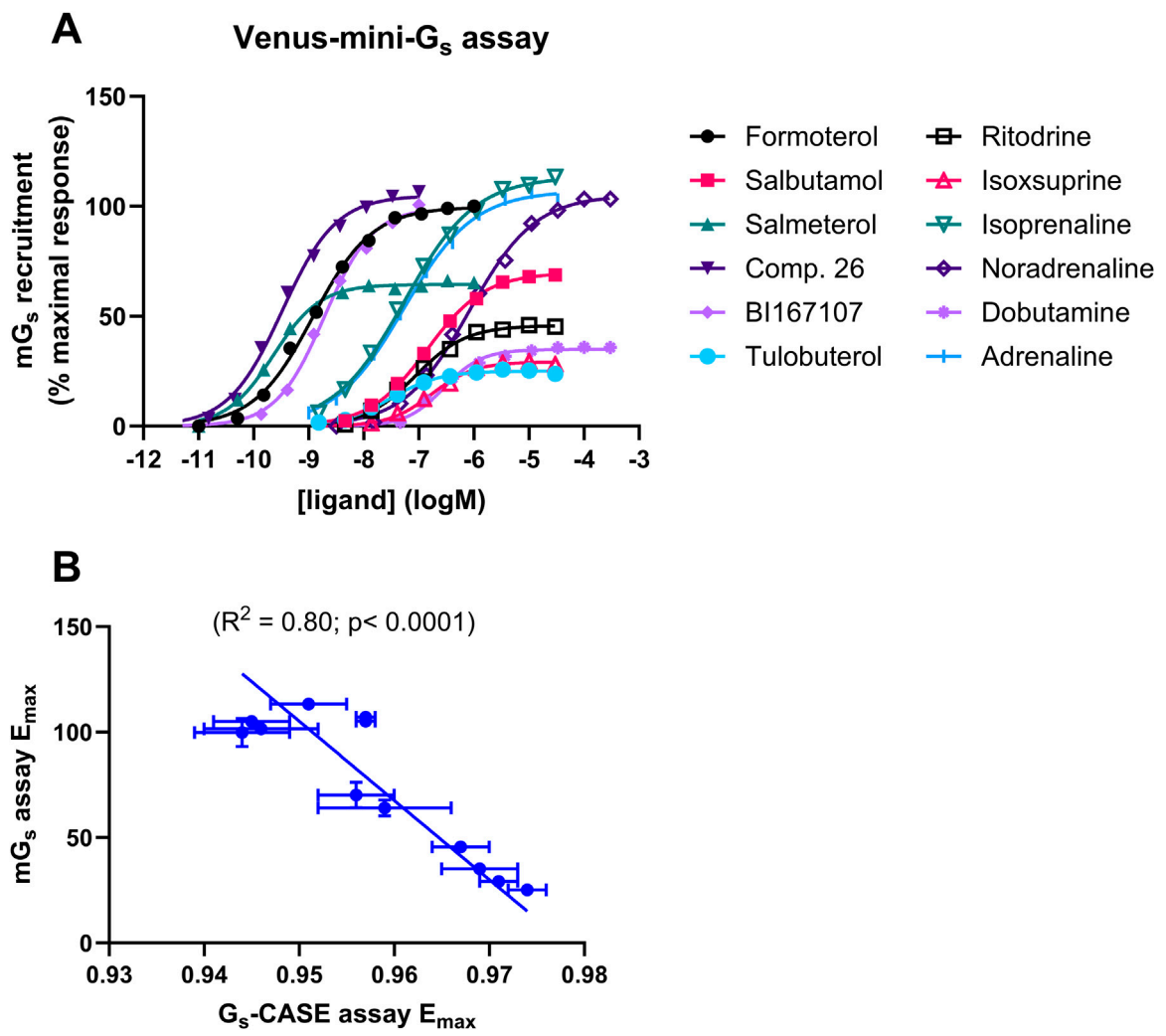

FIGURE 2
β_2AR ligand efficacy determined in the Venus-mini-G_s recruitment assay. **(A)** Ligand-induced increases in BRET, following the recruitment of Venus-labelled mini-G_s to β_2AR-nLuc. The Venus-mini-G_s ligand-response amplitude of each agonist was compared to the maximal response of formoterol (1 μM). **(B)** Correlation of the Gs-CASE assay-response amplitude, expressed as the maximal Δ (E_{max}) in the baseline BRET signal, with E_{max} measured in the mini-Gs recruitment assay. Data are presented as the mean ± SEM of three experiments.

Affinity and the rate of association of Venus-mini-Gs protein for β_2AR-nLuc correlated with agonist efficacy

Finally, we performed Pearson's correlation analysis between both the association rates (k_{on}) and dissociation rates (k_{off}) and the affinity (pK_d) values for Venus-mini-Gs binding agonist β_2AR–nLuc complexes vs. agonist efficacy, comparing both G_s-CASE and mini-G_s assay E_{max} values (Figure 5). This analysis showed a strong correlation between ligand efficacy (E_{max}) measured in both assay formats and mini-G_s association rates (k_{on}) (R^2 = 0.78, $p < 0.0001$ and R^2= 0.99, $p < 0.0001$ respectively; see Figures 5A, D) and between ligand efficacy (E_{max}) and mini-G_s affinity (pK_d) (R^2 0.70, p = 0.0007 and R^2 = 0.93, $p < 0.0001$, respectively; see Figures 5C, F). This suggests that the differences in agonist efficacy can be explained by agonist β_2AR complexes' ability to recruit the G_s protein. No correlation was observed between ligand efficacy (E_{max}) measured in either assay formats and mini-G_s dissociation rates (k_{off}) (R^2 = 0.06, p = 0.45 and R^2 = 0.16, p = 0.20, respectively; see Figures 5B, E).

We also performed this same correlation analysis between these mini-G_s kinetics values obtained in detergent micelles and G_s efficacy data obtained in the Gs-CASE assay and found a similar trend (Supplementary Figure 4).

Efficacy of β_2AR agonists does not correlate with ligand binding kinetics

Previous studies have suggested that for some GPCRs, there is a relationship between ligand efficacy and the dissociation rates of ligand binding (Sykes et al., 2009a; Guo et al., 2016). To investigate the correlations between ligand residence time and efficacy, we analyzed existing kinetic data. This analysis revealed a broad

TABLE 2 Summary of mini-Gs assay potency (pEC_{50}) and efficacy (E_{max}) values and literature pK_i values for the 12 agonists of varied efficacy under study.

	Mini-Gs recruitment assay		Radioligand binding
	pEC_{50}	E_{max} (% formoterol response)	pK_i or pK_d
Formoterol	8.92 ± 0.09	99.9 ± 6.7	8.63 ± 0.02
Salbutamol	6.85 ± 0.09	70.2 ± 6.0	6.01 ± 0.03
Salmeterol	9.64 ± 0.08	64.1 ± 3.8	9.26 ± 0.06
Compound 26	9.48 ± 0.03	105.1 ± 1.6	*9.81 ± 0.09
BI167107	9.48 ± 0.03	101.6 ± 0.83	**10.1
Tulobuterol	7.50 ± 0.04	25.1 ± 2.3	6.83 ± 0.09
Ritodrine	7.07 ± 0.08	45.6 ± 2.9	5.81 ± 0.07
Isoxsuprine	6.76 ± 0.14	29.2 ± 2.4	5.93 ± 0.09
Isoprenaline	7.27 ± 0.14	113.4 ± 2.0	6.64 ± 0.09
Noradrenaline	6.08 ± 0.06	105.1 ± 1.3	5.41 ± 0.07
Dobutamine	6.52 ± 0.08	35.2 ± 0.9	5.84 ± 0.05
Adrenaline	7.30 ± 0.08	107.0 ± 2.9	6.13 ± 0.05

The mini-Gs assay values are presented as the mean of three experiments ±SEM. Literature binding pK_i/pK_d values are taken from Baker (2010), Rasmussen et al. (2011a), Rosethorne et al. (2016), Baker (2010), Rosethorne et al. (2016), and Rasmussen et al. (2011b). The Venus-labelled mini-G_s ligand-response amplitude of each agonist was compared to the maximal response of formoterol (1 μM). Data are shown as the mean ± SEM of three experiments.

range of measured k_{off} values, with adrenaline exhibiting the fastest dissociation rate and Compound 26 showing the slowest.

The relationships between agonist efficacy, as determined by E_{max} values obtained from the Gs-CASE and mini-G_s recruitment assays, and literature ligand binding association (k_{on}) and dissociation rates (k_{off}) were determined using Pearson's correlation analysis (see Figure 6). This analysis showed no statistically significant correlation between ligand k_{off} values and the efficacy values determined for 6 of the 12 β_2AR agonists. Moreover, we also conducted kinetic TR-FRET-based ligand binding studies on 6 of the 12 β_2AR agonists in detergent micelles (Supplementary Figure 5) and found no statistically significant correlation (R^2 = 0.26, p = 0.29) between relative ligand residence times (IC_{50} 1 min/IC_{50} equilibrium) and their efficacy (Supplementary Figure 6; Supplementary Table 2).

Discussion

In this study, we aimed to investigate the molecular basis for ligand efficacy. The first hypothesis was that the ligand binding kinetics, or ligand residence time, may influence efficacy. The second hypothesis was that the kinetics of G protein recruitment to the receptor–agonist complex may be correlated to ligand efficacy.

We found no correlations between the ligand binding kinetics and its efficacy. Whilst some studies suggested a role for ligand dissociation kinetics (Guo et al., 2012; Sykes et al., 2009) for adenosine $A2_A$ and muscarinic M_3 receptors, our data are congruent with the previously reported observation that it was not the case for β_2AR (Sykes and Charlton, 2012).

Alternatively, we observed a linear correlation between ligand-induced differences in mini-G_s protein binding kinetics (k_{on}) and affinity (pK_d) for the agonist-bound β_2AR and agonist efficacy, the ability of a ligand to activate the heterotrimeric G_s protein. In contrast, our data showed minimal difference in the dissociation rate (k_{off}) or corresponding residence time ($1/k_{off}$) of the Venus-mini-G_s when binding to different agonist-β_2AR complexes. Since the affinity of mini-G_s is a ratio of k_{on} and k_{off} and mini-G_s k_{off} appears relatively constant, it is expected that mini-G_s k_{on} and its affinity correlate.

Our hypothesis is that agonist binding to the β_2AR increases the propensity for G protein recruitment, which underlies the molecular basis of ligand efficacy at the β_2AR (Figure 7A). To support our hypothesis, we applied a previously validated mathematical model of the cubic ternary complex model (BioModels ID:2306220001) to investigate the effect of increasing the forward rate of G protein binding to the activated receptor, on both G protein activation and agonist–receptor occupancy at the β_2AR (Figures 7B, C). As indicated, increasing the on-rate for G protein recruitment increases the efficacy and potency of G protein activation by the ligand, without changing agonist–receptor occupancy (Figure 7B). This, therefore, supports our hypothesis that an increase in G protein recruitment propensity underlies the molecular basis of ligand efficacy at the β_2AR.

These differences in the rate of mini-G_s recruitment and the resulting differences in mini-G_s affinity suggest that subtle differences in agonist β_2AR complex conformations result in differences in agonist efficacy due of differences in the ability of these conformations to affect the recruitment of Venus-mini-G_s. As the dissociation rates of the mini-G_s protein are very similar for all ligands, the structure of the GPCR–G protein complex is likely similar for all ligands. This hypothesis aligns with recent observations made by NMR (Jones et al., 2024), where the full agonist isoprenaline induced a different conformational state of the β_1 adrenergic receptor (β_1AR) compared to the partial agonists xamoterol and salbutamol. However, the conformations were

10.3389/fphar.2025.1367991

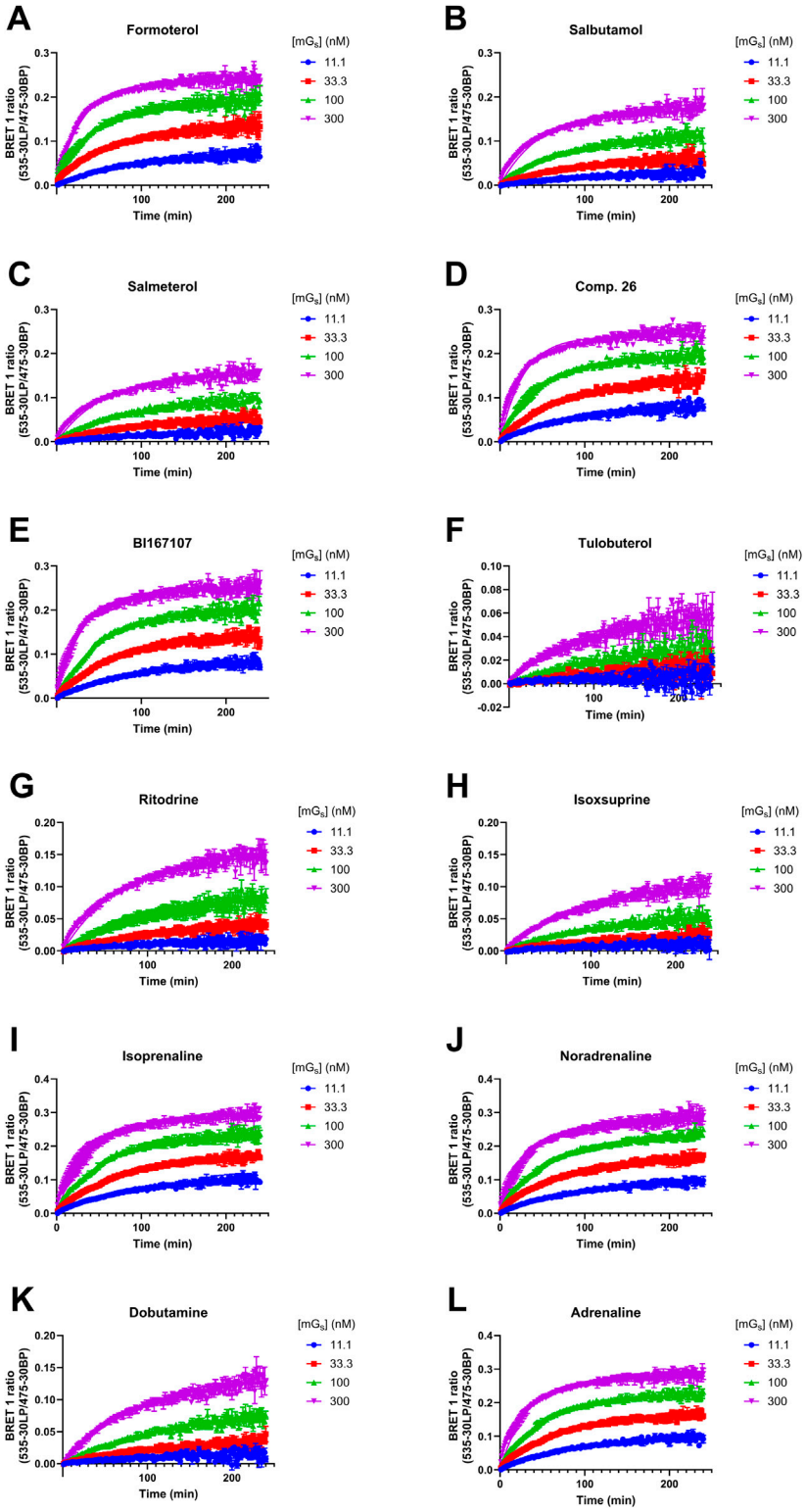

FIGURE 3
Kinetics of the association of Venus-mini-G_s to the agonist β_2AR–nLuc complex, as measured using nanoBRET. Recruitment of the mini-G_s protein by **(A)** formoterol, **(B)** salbutamol, **(C)** salmeterol, **(D)** Compound 26, **(E)** BI167107, **(F)** tulobuterol, **(G)** ritodrine, **(H)** isoxsuprine, **(I)** isoprenaline, **(J)** noradrenaline, **(K)** dobutamine, and **(L)** adrenaline. Data are presented as the mean ± SEM of three experiments.

TABLE 3 Summary of mean k_{off}, k_{on}, and K_d values for purified Venus-mini-G_s recruitment to TS-SNAP-β_2AR-nLuc by various β_2AR agonists; NanoBRET between TS-SNAP-β_2AR-nLuc and Venus-mini-G_s read on PHERAstar FSX, at room temperature, using the BRET1 module.

	Mini-G_s recruitment assay		
	Mini-G_s k_{off} (min^{-1})	Mini-G_s k_{on} (M^{-1} min^{-1})	Mini-G_s K_d (nM)
Formoterol	0.0084 ± 0.0003	2.77 ± 0.09 × 10^5	30.4 ± 2.0
Salbutamol	0.0113 ± 0.0003	1.16 ± 0.04 × 10^5	97.5 ± 5.9
Salmeterol	0.0109 ± 0.0007	9.18 ± 1.24 × 10^4	126 ± 27
Compound 26	0.0076 ± 0.0007	2.73 ± 0.13 × 10^5	27.8 ± 1.2
BI167107	0.0070 ± 0.0002	2.58 ± 0.07 × 10^5	27.1 ± 1.3
Tulobuterol	0.0073 ± 0.0015	4.43 ± 0.39 × 10^4	161 ± 21
Ritodrine	0.0107 ± 0.0004	6.13 ± 0.75 × 10^4	182 ± 32
Isoxsuprine	0.0096 ± 0.0011	4.97 ± 0.29 × 10^4	193 ± 11
Isoprenaline	0.0073 ± 0.0003	3.00 ± 0.11 × 10^5	24.5 ± 1.6
Noradrenaline	0.0076 ± 0.0012	2.99 ± 0.25 × 10^5	25.0 ± 2.0
Dobutamine	0.0008 ± 0.0007	6.16 ± 0.26 × 10^4	133 ± 5
Adrenaline	0.0077 ± 0.0006	3.06 ± 0.15 × 10^5	25.1 ± 0.1

Values are presented as the mean ± SEM of three independent experiments.

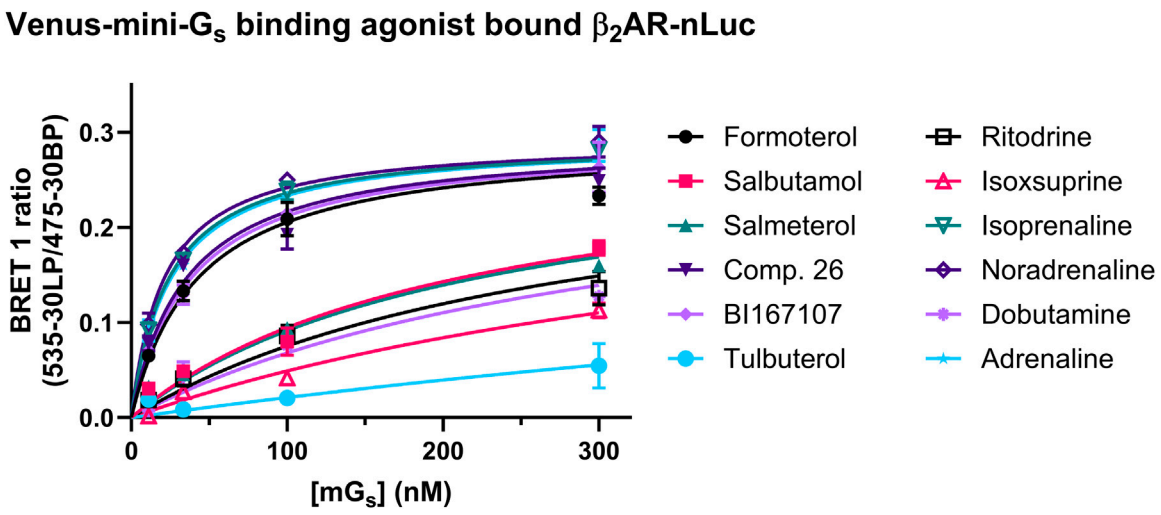

FIGURE 4
Equilibrium binding of Venus-mini-G_s bound to β_2AR-nLuc at saturating concentrations of each agonist, as reflected by an increase in the BRET signal. The full agonist β_2AR complexes recruit Venus-mini-G_s with higher affinity compared to partial agonist β_2AR mG complexes. Data shown are presented as the mean ± SEM of three experiments.

similar in the case of the ternary complex with mini-G_s. The authors also reported faster recruitment kinetics for the full agonist isoprenaline, a result that aligns well with our own observations for a wide range of partial and full agonists, as presented in this study.

Moreover, this conformational model (see Figure 7) is supported by data from hydrogen/deuterium exchange mass spectrometry (HDMS) and hydroxy radical foot printing mass spectrometry (HDX) (Du et al., 2019), where the conformational changes involved in β_2AR–G_s protein complex formation were investigated. Du et al. showed that the conformation of the initial β_2AR–G_s structure differs from that of the fully formed nucleotide free β_2AR–G_s complex. Furthermore, NMR studies (Nygaard et al., 2013; Manglik et al., 2015) show that the agonist BI-167-107 alone is not sufficient to fully stabilise the β_2AR in the active state and that nanobody 80 is required to fully stabilise the active state. These data support our findings that the conformation of the agonist β_2AR complex differs from that of the agonist β_2AR–mini-G_s complex.

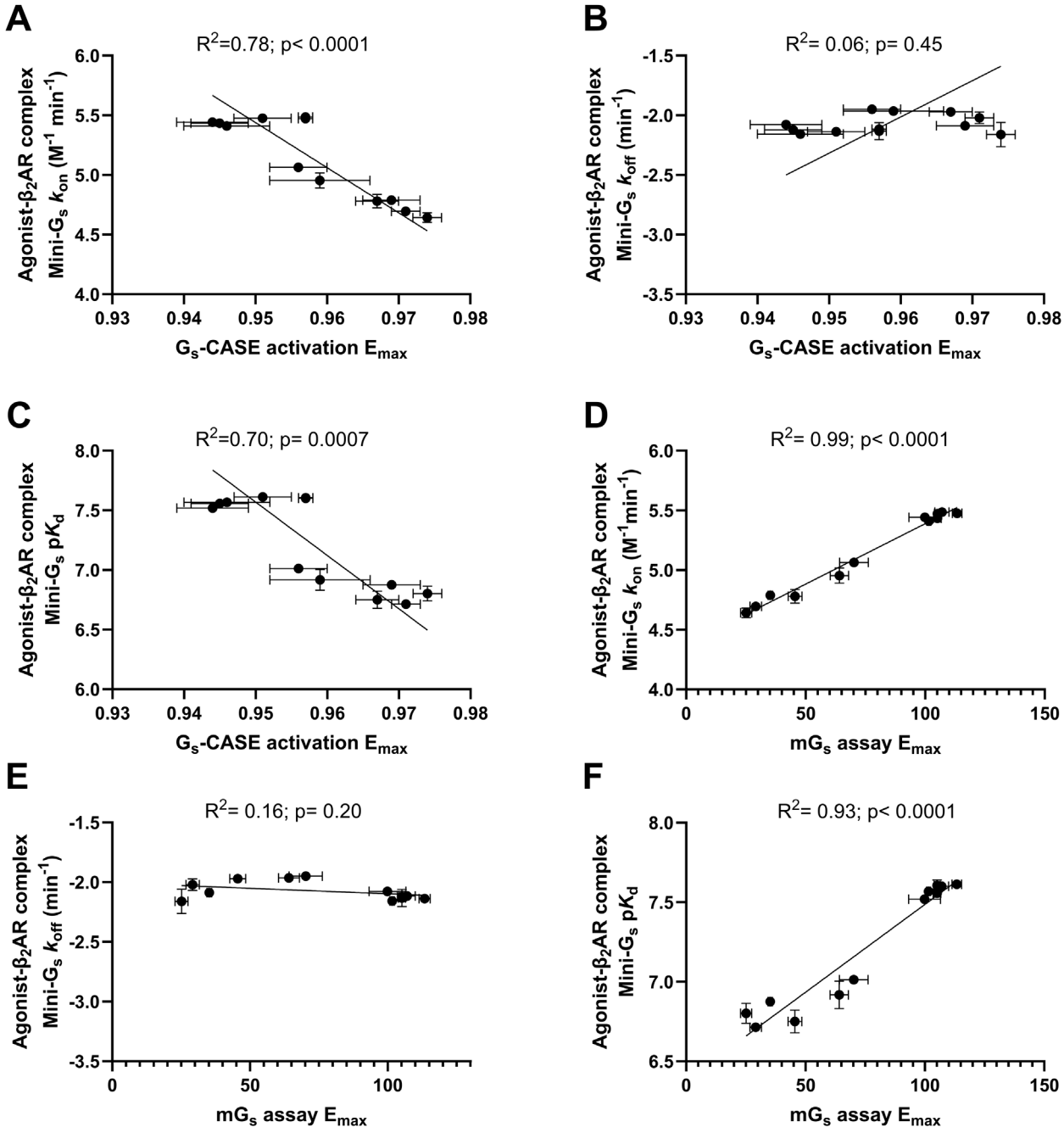

FIGURE 5
Correlation plots of G_s-CASE activation E_{max} with **(A)** agonist β_2AR complex Venus-mini-G_s association rate (k_{on}), **(B)** β_2AR complex Venus-mini-G_s affinity (pK_d), and **(C)** β_2AR complex Venus-mini-G_s dissociation rate (k_{off}). The GS-CASE response to each agonist is expressed as a fractional change relative to the basal response. Correlation plots of mini-G_s assay E_{max} with **(D)** agonist β_2AR complex Venus-mini-G_s association rate (k_{on}), **(E)** β_2AR complex Venus-mini-G_s affinity (pK_d), and **(F)** β_2AR complex Venus-mini-G_s dissociation rate (k_{off}). The Venus-labelled mini-G_s ligand-response amplitude of each agonist in the mini-G_s assay was compared to the maximal response of formoterol (1 μM). Deming regression was applied to determine the line of best fit. Data are shown as the mean ± SEM of three experiments.

Moreover, Liu et al. (2012) investigated the conformational states of β_2AR bound to agonists of a range of efficacies and showed efficacy-dependent differences in the agonist β_2AR conformational state. Structural studies of the agonist-bound β_2AR or other class A GPCRs have only been possible in the presence of a G protein mimetics (Rasmussen et al., 2011b) and show only very small conformational differences that do not seem to explain differences in efficacy (Katritch et al., 2009). This further supports our finding that there was no difference in the agonist β_2AR–mini-G_s complex conformation.

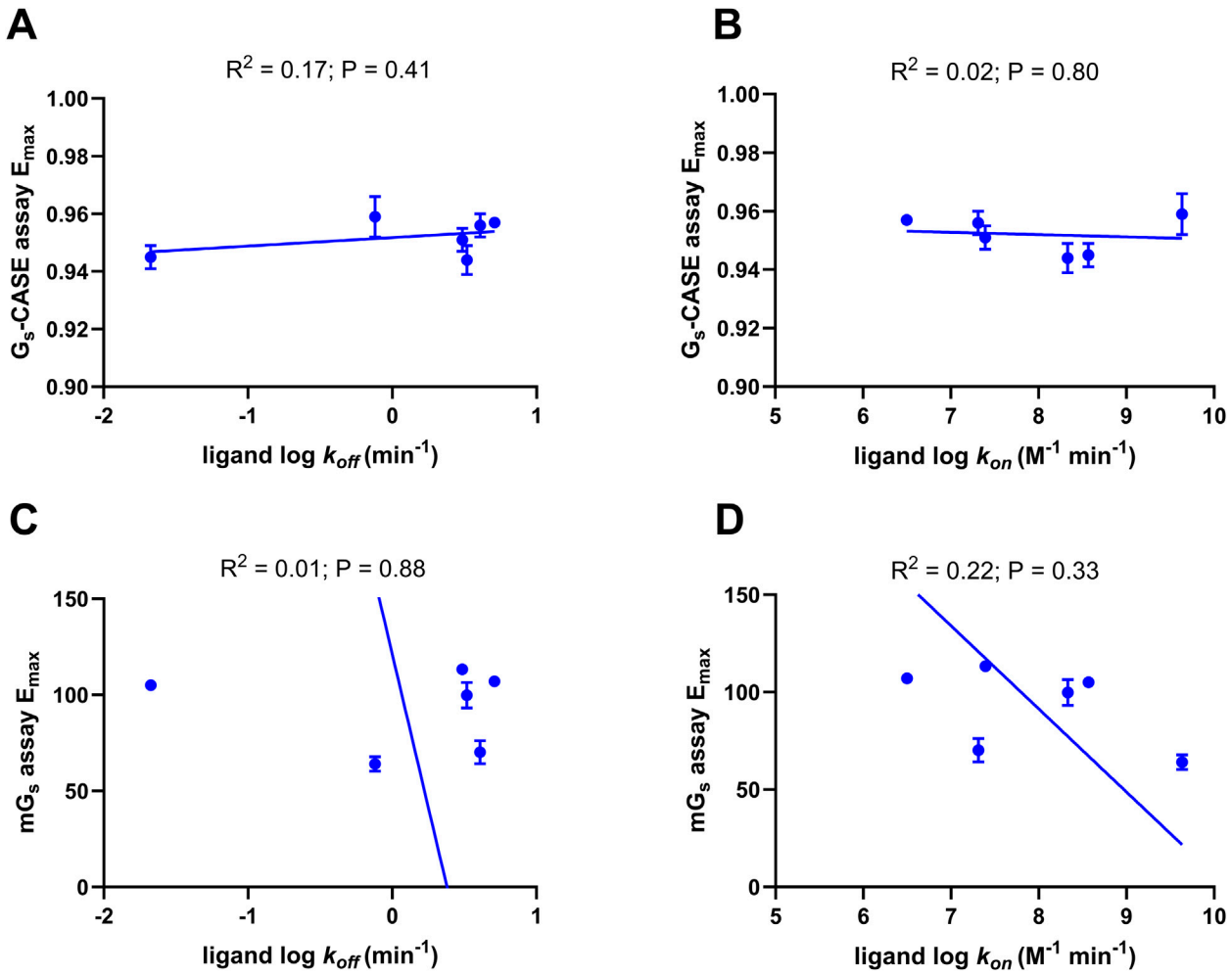

FIGURE 6
Correlation plots of ligand efficacy with ligand binding parameters. Plot of **(A)** ligand dissociation rates (k_{off}) with G_s-CASE activation E_{max} and **(B)** ligand association rate (k_{on}) with G_s-CASE activation E_{max}. The Gs-CASE assay response amplitude is expressed as the maximal Δ (E_{max}) in the baseline BRET signal, which was set to 1.0. Plot of **(C)** ligand dissociation rates (k_{off}) with mini-G_s assay E_{max} and **(D)** ligand association rate (k_{on}) with mini-G_s assay E_{max}. The Venus-labelled mini-G_s ligand-response amplitude of each agonist in the mini-G_s assay was compared to the maximal response of formoterol (1 μM). Deming regression was applied to determine the line of best fit. Data are shown as the mean ± SEM of three experiments. Ligand association and dissociation rates were taken from Sykes et al., 2014, Sykes et al., 2012 and Rosethorne et al., 2016.

We performed the majority of this study in membranes as we believe this environment is the most physiologically relevant for performing a kinetic analysis of ligand-induced mini-G_s binding. We also reproduced most of the experiments with receptor isolated in DDM detergent micelles (Supplementary Figures 2–6); this approach gives us confidence that our conclusions are relevant purely at the biophysical level, independent of the regulatory elements of the cell, while also establishing a baseline for future biophysical studies. However, the full applicability of our findings to the native cell environment remains to be fully elucidated. Interestingly, Sungkaworn et al. (2017) investigated the association rate (k_{on}) and dissociation rate (k_{off}) of $G\alpha_I$ binding to the α2AR receptor in CHO cells in response to a range of agonists using single molecule microscopy. They showed that efficacy is at least partially correlated with k_{on} but not k_{off} of the $G\alpha_I$ protein. Taken together with the evidence from the current study, this suggests that the conformational model of efficacy proposed may extend to the cellular environment. Future work will investigate whether this model of efficacy proposed is relevant to the β_2AR in its native cellular environment and whether this model can be generalized as a mechanism for agonist efficacy at other GPCRs.

Conclusion

In summary, these findings suggest that differences in initial agonist-GPCR conformations, where full agonists stabilise a state that readily recruits G protein, could be central to understanding the molecular basis of efficacy for the 12 β_2AR agonists studied. In contrast, we found no evidence linking ligand or G protein binding dissociation kinetics to the molecular basis of ligand efficacy at the β_2AR. We propose a conformational model of efficacy, in which

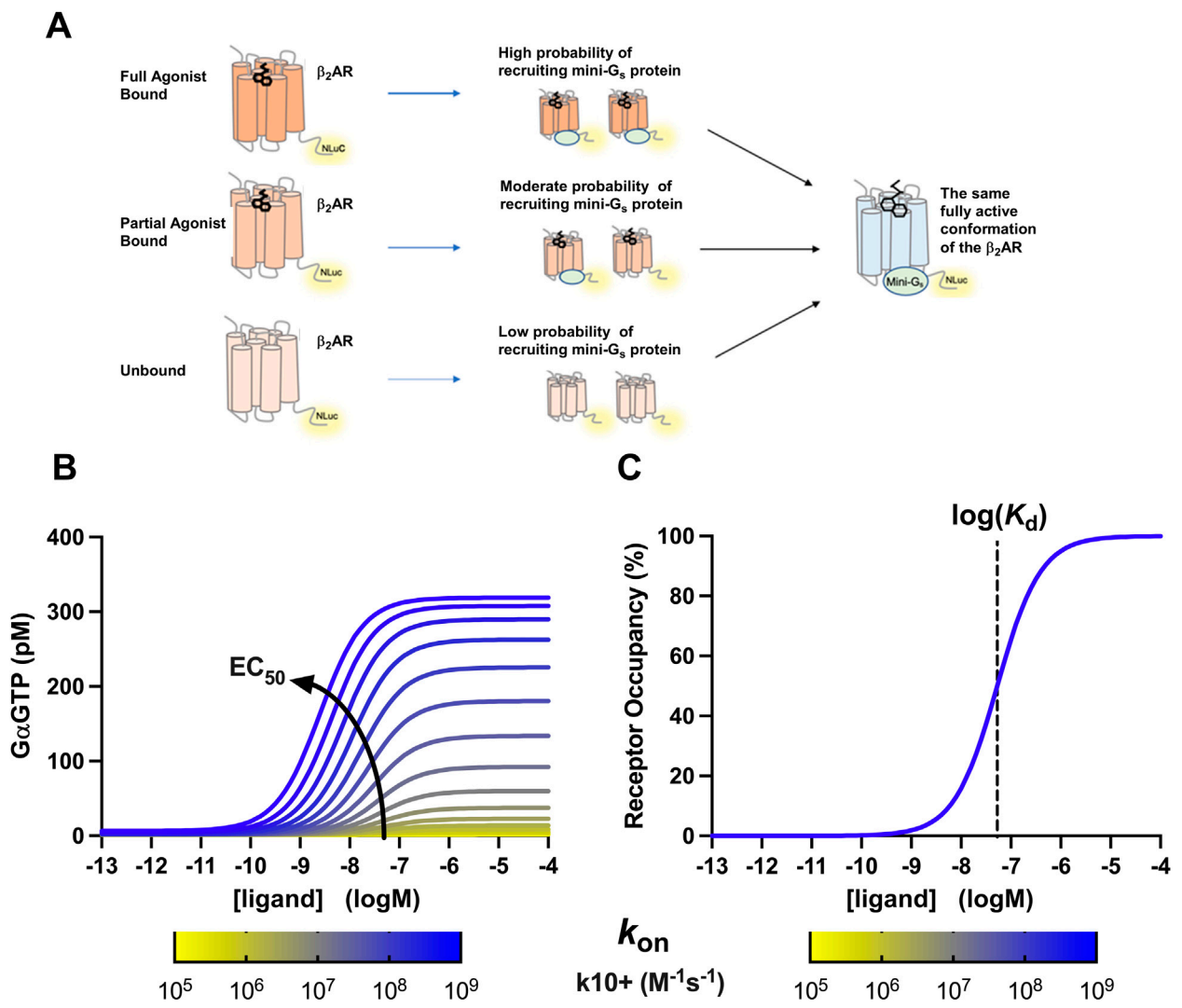

FIGURE 7
Conformational model of efficacy proposed by this study: **(A)** agonists of higher efficacy induce a conformation of β_2AR that is more likely to recruit a mini-G_s protein, but once bound, there is no difference in the β_2AR conformation within the agonist β_2AR-mini–G_s complex. **(B)** Use of the cubic ternary complex model to investigate the effect of increasing the rate of G protein recruitment on the potency of the agonist–receptor complex to activate the G protein. Arrow indicates increases in apparent ligand EC_{50} values for the formation of GαGTP. **(C)** Use of the cubic ternary complex model to investigate the effect of increasing the rate of G protein recruitment on agonist affinity for the GPCR. Dotted line indicates log (K_d) of ligand-receptor occupancy. As shown in the figure, the association rate of Gα to the receptor does not affect ligand binding affinity; hence, the yellow and blue curves lie directly on top of each other.

agonists with higher efficacy stabilise a conformation of β_2AR that is more likely to recruit the G protein. The results from mini-G protein association experiments with ligand prebound to the receptor provide a convenient and direct measurement of ligand efficacy. Further studies incorporating a broader range of agonists with varying efficacies, along with measurements across different receptor types, would help determine whether this mechanism is a general feature of GPCR efficacy.

Data availability statement

The raw data supporting the conclusions of this article will be made available by the authors, without undue reservation.

Ethics statement

Ethical approval was not required for the studies on humans in accordance with the local legislation and institutional requirements because only commercially available established cell lines were used. Ethical approval was not required for the studies on animals in accordance with the local legislation and institutional requirements because only commercially available established cell lines were used.

Author contributions

CH. DS: formal analysis and writing–review and editing. TR-N: investigation, methodology, resources, writing–original draft, and

writing–review and editing. OU, CN, AK, EK, and GL: conceptualization, supervision, writing–original draft, and writing–review and editing. SB: conceptualization, funding acquisition, supervision, writing–original draft, and writing–review and editing. DV: conceptualization, funding acquisition, resources, supervision, writing–original draft, and writing–review and editing.

Funding

The author(s) declare that financial support was received for the research and/or publication of this article. CH was funded by a Medical Research Council (MRC) IMPACT PhD studentship. TR-N was funded by a UK Biotechnology and Biological Sciences Research Council iCase studentship (BB/V509334/1) co-funded with AstraZeneca. AK is funded by the BBSRC Doctorate Training Program at the University of Nottingham. GL is a Royal Society Industry Fellow (NF\R2\212001). EK, CN, DS and DV gratefully acknowledge funding by the Medical Research Council [grant number MR/Y003667/1] and Biotechnology and Biological Sciences Research Council [BB/Y51407X/1] and [BB/Z514500/1].

Acknowledgments

The authors would like to thank Dr. Bradley Hoare and Dr. Franziska M. Heydenreich for, respectively, generating the pcDNA4TO-TS-SNAP-β_2AR-nLuc and pcDNA4TO-TS-SNAP-β_2AR and Nevin Lambert for sharing the templates for Venus-mG plasmids used in this study.

Conflict of interest

DS and DV are founding directors of Z7 Biotech Ltd., an early-stage drug discovery company. OU is an employee of Z7 Biotech Ltd.

The remaining authors declare that the research was conducted in the absence of any commercial or financial relationships that could be construed as a potential conflict of interest.

Publisher's note

Supplementary material

The Supplementary Material for this article can be found online at: https://www.frontiersin.org/articles/10.3389/fphar.2025.1367991/full#supplementary-material

References

Baker, J. G. (2010). The selectivity of beta-adrenoceptor agonists at human beta1-beta2- and beta3-adrenoceptors. *Br. J. Pharmacol.* 160 (5), 1048–1061. doi:10.1111/j.1476-5381.2010.00754.x

Bridge, L. J., Mead, J., Frattini, E., Winfield, I., and Ladds, G. (2018). Modelling and simulation of biased agonism dynamics at a G protein-coupled receptor. *J. Theor. Biol.* 442, 44–65. doi:10.1016/j.jtbi.2018.01.010

Carpenter, B., Nehme, R., Warne, T., Leslie, A. G., and Tate, C. G. (2016). Structure of the adenosine A(2A) receptor bound to an engineered G protein. *Nature* 536 (7614), 104–107. doi:10.1038/nature18966

Carpenter, B., and Tate, C. G. (2016). Engineering a minimal G protein to facilitate crystallisation of G protein-coupled receptors in their active conformation. *Protein Eng. Des. Sel.* 29 (12), 583–594. doi:10.1093/protein/gzw049

Carpenter, B., and Tate, C. G. (2017). Expression, purification and crystallisation of the adenosine A(2A) receptor bound to an engineered mini G protein. *Bio Protoc.* 7 (8), e2234. doi:10.21769/BioProtoc.2234

Deupi, X., and Kobilka, B. K. (2010). Energy landscapes as a tool to integrate GPCR structure, dynamics, and function. *Physiol. (Bethesda)* 25 (5), 293–303. doi:10.1152/physiol.00002.2010

Du, Y., Duc, N. M., Rasmussen, S. G. F., Hilger, D., Kubiak, X., Wang, L., et al. (2019). Assembly of a GPCR-G protein complex. *Cell* 177 (5), 1232–1242. doi:10.1016/j.cell.2019.04.022

Grahl, A., Abiko, L. A., Isogai, S., Sharpe, T., and Grzesiek, S. (2020). A high-resolution description of β1-adrenergic receptor functional dynamics and allosteric coupling from backbone NMR. *Nat. Commun.* 11 (1), 2216. doi:10.1038/s41467-020-15864-y

Gregorio, G. G., Masureel, M., Hilger, D., Terry, D. S., Juette, M., Zhao, H., et al. (2017). Single-molecule analysis of ligand efficacy in β2AR-G-protein activation. *Nature* 547 (7661), 68–73. doi:10.1038/nature22354

Guo, D., Heitman, L. H., and Ap, I. J. (2016). The added value of assessing ligand-receptor binding kinetics in drug discovery. *ACS Med. Chem. Lett.* 7 (9), 819–821. doi:10.1021/acsmedchemlett.6b00273

Guo, D., Mulder-Krieger, T., Ijzerman, A. P., and Heitman, L. H. (2012). Functional efficacy of adenosine A_2A receptor agonists is positively correlated to their receptor residence time. *Br. J. Pharmacol.* 166 (6), 1846–1859. doi:10.1111/j.1476-5381.2012.01897.x

Harwood, C. R., Sykes, D. A., Redfern-Nichols, T., Ladds, G., Briddon, S. J., and Veprintsev, D. B. (2024). Agonist efficacy at the β_2AR is driven by agonist-induced differences in receptor affinity for the G_s protein, not ligand binding kinetics. *bioRxiv* 2024. 2001.2005.574357. doi:10.1101/2024.01.05.574357

Hauser, A. S., Attwood, M. M., Rask-Andersen, M., Schioth, H. B., and Gloriam, D. E. (2017). Trends in GPCR drug discovery: new agents, targets and indications. *Nat. Rev. Drug Discov.* 16 (12), 829–842. doi:10.1038/nrd.2017.178

Heydenreich, F. M., Miljus, T., Jaussi, R., Benoit, R., Milic, D., and Veprintsev, D. B. (2017). High-throughput mutagenesis using a two-fragment PCR approach. *Sci. Rep.* 7 (1), 6787. doi:10.1038/s41598-017-07010-4

Hoops, S., Sahle, S., Gauges, R., Lee, C., Pahle, J., Simus, N., et al. (2006). COPASI--a COmplex PAthway SImulator. *Bioinformatics* 22 (24), 3067–3074. doi:10.1093/bioinformatics/btl485

Jones, A. J. Y., Harman, T. H., Harris, M., Lewis, O. E., Ladds, G., and Nietlispach, D. (2024). Binding kinetics drive G protein subtype selectivity at the β1-adrenergic receptor. *Nat. Commun.* 15 (1), 1334. doi:10.1038/s41467-024-45680-7

Katritch, V., Reynolds, K. A., Cherezov, V., Hanson, M. A., Roth, C. B., Yeager, M., et al. (2009). Analysis of full and partial agonists binding to beta2-adrenergic receptor suggests a role of transmembrane helix V in agonist-specific conformational changes. *J. Mol. Recognit.* 22 (4), 307–318. doi:10.1002/jmr.949

Liu, J. J., Horst, R., Katritch, V., Stevens, R. C., and Wuthrich, K. (2012). Biased signaling pathways in β2-adrenergic receptor characterized by 19F-NMR. *Science* 335 (6072), 1106–1110. doi:10.1126/science.1215802

Louvel, J., Guo, D., Agliardi, M., Mocking, T. A. M., Kars, R., Pham, T. P., et al. (2014). Agonists for the adenosine A1 receptor with tunable residence time. A case for nonribose 4-Amino-6-aryl-5-cyano-2-thiopyrimidines. *J. Med. Chem.* 57 (8), 3213–3222. doi:10.1021/jm401643m

Manglik, A., Kim, T. H., Masureel, M., Altenbach, C., Yang, Z., Hilger, D., et al. (2015). Structural insights into the dynamic process of β2-adrenergic receptor signaling. *Cell* 161, 1101–1111. doi:10.1016/j.cell.2015.04.043

Mary, S., Damian, M., Louet, M., Floquet, N., Fehrentz, J. A., Marie, J., et al. (2012). Ligands and signaling proteins govern the conformational landscape explored by a G protein-coupled receptor. *Proc. Natl. Acad. Sci. U. S. A.* 109, 8304–8309. doi:10.1073/pnas.1119881109

Masureel, M., Zou, Y., Picard, L.-P., van der Westhuizen, E., Mahoney, J. P., Rodrigues, J. P. G. L. M., et al. (2018). Structural insights into binding specificity, efficacy and bias of a β2AR partial agonist. *Nat. Chem. Biol.* 14 (11), 1059–1066. doi:10.1038/s41589-018-0145-x

Nikolaev, V. O., Hoffmann, C., Bünemann, M., Lohse, M. J., and Vilardaga, J.-P. (2006). Molecular basis of partial agonism at the neurotransmitter alpha2A-adrenergic receptor and Gi-protein heterotrimer. *J. Biol. Chem.* 281 (34), 24506–24511. doi:10.1074/jbc.M603266200

Nygaard, R., Zou, Y., Dror, R. O., Mildorf, T. J., Arlow, D. H., Manglik, A., et al. (2013). The dynamic process of β(2)-adrenergic receptor activation. *Cell* 152 (3), 532–542. doi:10.1016/j.cell.2013.01.008

Rasmussen, S. G., Choi, H. J., Fung, J. J., Pardon, E., Casarosa, P., Chae, P. S., et al. (2011a). Structure of a nanobody-stabilized active state of the β(2) adrenoceptor. *Nature* 469 (7329), 175–180. doi:10.1038/nature09648

Rasmussen, S. G., DeVree, B. T., Zou, Y., Kruse, A. C., Chung, K. Y., Kobilka, T. S., et al. (2011b). Crystal structure of the β2 adrenergic receptor-Gs protein complex. *Nature* 477 (7366), 549–555. doi:10.1038/nature10361

Rosethorne, E. M., Bradley, M. E., Gherbi, K., Sykes, D. A., Sattikar, A., Wright, J. D., et al. (2016). Long receptor residence time of C26 contributes to super agonist activity at the human β2 adrenoceptor. *Mol. Pharmacol.* 89 (4), 467–475. doi:10.1124/mol.115.101253

Schihada, H., Shekhani, R., and Schulte, G. (2021). Quantitative assessment of constitutive G protein–coupled receptor activity with BRET-based G protein biosensors. *Sci. Signal.* 14 (699), eabf1653. doi:10.1126/scisignal.abf1653

Sun, D., Flock, T., Deupi, X., Maeda, S., Matkovic, M., Mendieta, S., et al. (2015). Probing Gαi1 protein activation at single-amino acid resolution. *Nat. Struct. Mol. Biol.* 22 (9), 686–694. doi:10.1038/nsmb.3070

Sungkaworn, T., Jobin, M.-L., Burnecki, K., Weron, A., Lohse, M. J., and Calebiro, D. (2017). Single-molecule imaging reveals receptor–G protein interactions at cell surface hot spots. *Nature* 550 (7677), 543–547. doi:10.1038/nature24264

Sykes, D. A., and Charlton, S. J. (2012). Slow receptor dissociation is not a key factor in the duration of action of inhaled long-acting β2-adrenoceptor agonists. *Br. J. Pharmacol.* 165 (8), 2672–2683. doi:10.1111/j.1476-5381.2011.01639.x

Sykes, D. A., Dowling, M. R., and Charlton, S. J. (2009a). Exploring the mechanism of agonist efficacy: a relationship between efficacy and agonist dissociation rate at the muscarinic M3 receptor. *Mol. Pharmacol.* 76 (3), 543–551. doi:10.1124/mol.108.054452

Sykes, D. A., Dowling, M. R., and Charlton, S. J. (2009b). Exploring the mechanism of agonist efficacy: a relationship between efficacy and agonist dissociation rate at the muscarinic M3 receptor. *Mol. Pharmacol.* 76 (3), 543–551. doi:10.1124/mol.108.054452

Sykes, D. A., Parry, C., Reilly, J., Wright, P., Fairhurst, R. A., and Charlton, S. J. (2014). Observed drug-receptor association rates are governed by membrane affinity: the importance of establishing "micro-pharmacokinetic/pharmacodynamic relationships" at the β2-adrenoceptor. *Mol. Pharmacol.* 85 (4), 608–617. doi:10.1124/mol.113.090209

Wan, Q., Okashah, N., Inoue, A., Nehmé, R., Carpenter, B., Tate, C. G., et al. (2018). Mini G protein probes for active G protein–coupled receptors (GPCRs) in live cells. *J. Biol. Chem.* 293 (19), 7466–7473. doi:10.1074/jbc.RA118.001975

Weiss, J. M., Morgan, P. H., Lutz, M. W., and Kenakin, T. P. (1996). The cubic ternary complex receptor-occupancy model. III. resurrecting efficacy. *J. Theor. Biol.* 181 (4), 381–397. doi:10.1006/jtbi.1996.0139

Woodroffe, P. J., Bridge, L. J., King, J. R., and Hill, S. J. (2009). Modelling the activation of G-protein coupled receptors by a single drug. *Math. Biosci.* 219 (1), 32–55. doi:10.1016/j.mbs.2009.02.003

Ye, L., Van Eps, N., Zimmer, M., Ernst, O. P., and Prosser, R. S. (2016). Activation of the A2A adenosine G-protein-coupled receptor by conformational selection. *Nature* 533 (7602), 265–268. doi:10.1038/nature17668

Zhang, Y., Yang, F., Ling, S., Lv, P., Zhou, Y., Fang, W., et al. (2020). Single-particle cryo-EM structural studies of the β2AR-Gs complex bound with a full agonist formoterol. *Cell Discov.* 6 (1), 45. doi:10.1038/s41421-020-0176-9